Electronic Supplementary Information for

Asymmetric liquid crystalline donors with two different end groups enable efficient all-small-molecule organic solar cells

Chenhe Wang,‡[a] Tianyi Chen,‡[a] Shuixing Li,[b] Yecheng Shen,[a] Jinyang Yu,[a] Adiljan Wupur,[a] Yongmin Luo,[c] Mengting Wang,[a] Xiukun Ye,[a] Jiaying Wu,[c] Minmin Shi*[a]* and *Hongzheng Chen*[a,b]*

[a] State Key Laboratory of Silicon and Advanced Semiconductor Materials, MOE Key Laboratory of Macromolecular Synthesis and Functionalization, Department of Polymer Science and Engineering, Zhejiang University, Hangzhou 310058, P. R. China. E-mail: minminshi@zju.edu.cn; hzchen@zju.edu.cn

[b] Zhejiang University-Hangzhou Global Scientific and Technological Innovation Center, Hangzhou 311200, P. R. China. Email: lishuixing89@zju.edu.cn

[c] The Hong Kong University of Science and Technology (Guangzhou), Function Hub, Advanced Materials Thrust, Nansha, Guangzhou 511400, P. R. China.

‡ C. Wang and T. Chen contributed equally to this work.

Materials Synthesis

All the reagents, unless otherwise specified, were purchased from Sigma-Aldrich Co., J&K, and Tokyo Chemical Industry Co., Ltd., and were used without further purification. The general synthetic routes for small molecules are shown in **Scheme 1.** BT-CAR2, BT-CAR4, and BT-CAR6 were obtained by the same synthetic process, and here we provide the synthesis route of BT-CAR2 as an example.

Synthesis of Compound 3: compound **1** (900 mg, 0.92 mmol), compound **2** (1200 mg, 2.29 mmol), and $Pd(PPh_3)_4$ (32.8 mg, 0.028 mmol) were added in anhydrous toluene (20 mL). The mixture was stirred at 110 ℃ for 36 h under argon protection and then cooled to room temperature. Then the mixture was quenched with cold deionized water and extracted with chloroform three times. The combined organic layer was washed with deionized water and dried over anhydrous sodium sulfate. After removal of the solvent, the crude product was purified by column chromatography over silica gel (eluent: petroleum ether: trichloromethane =2: 1 to give compound **3** as orange-red solid (860 mg, yield: 61.2%).^{1}H NMR (400 MHz, Chloroform-d) δ: 9.88 (s, 2H), 7.71 (d, J = 4.0 Hz, 2H), 7.55 (s, 2H), 7.25 (s, 2H), 7.23 (s, 1H), 7.22 (s, 1H), 7.12 (s, 2H), 7.02 (s, 2H), 2.91 – 2.74 (m, 12H), 1.78 (p, J = 6.3 Hz, 2H), 1.73 – 1.64 (m, 8H), 1.51 – 1.30 (m, 41H), 1.02 – 0.88 (m, 24H).

Synthesis of Compound 4: Compound 3 (800 mg, 0.523 mmol) and 2-ethylhexyl cyanoacetate (103 mg, 0.523 mmol) were added into a flask with 3 necks. 20 mL $CHCl_3$ and 0.5 mL piperidine were then added. After stirring at room temperature for 2 h, the obtained mixture was quenched with cold deionized water and extracted with chloroform three times. The combined organic layer was washed with deionized water and dried over anhydrous sodium sulfate. After removal of the solvent, the crude product was purified by column chromatography over silica gel (eluent: petroleum ether: trichloromethane =1: 1 to give compound **4** as black solid (380 mg, yield: 42.6%).^{1}H NMR (400 MHz, Chloroform-d) δ: 9.88 (s, 1H), 8.24 (s, 1H), 7.76 (d, J = 4.1 Hz, 1H), 7.71 (d, J = 4.0 Hz, 1H), 7.55 (s, 2H), 7.25 (s, 2H), 7.23 (dd, J = 4.0,

2.0 Hz, 2H), 7.12 (s, 2H), 7.02 (d, J = 2.2 Hz, 2H), 4.22 (dd, J = 5.8, 2.2 Hz, 2H), 2.91 – 2.74 (m, 12H), 1.78 (q, J = 6.3 Hz, 2H), 1.75 – 1.65 (m, 9H), 1.49 – 1.24 (m, 50H), 1.02 – 0.87 (m, 30H).

Synthesis of Compound BT-CAR2:

Compound 4 (100 mg, 0.06 mmol) and 3-Ethylrhodanine (48.3 mg, 0.3mmol) and ammonium acetate (100 mg) were added into a mix solution of chloroform/acetic acid (10 mL / 5 mL), and the mixture was heated to 100 °C and stirred for 4 h. The reaction mixture was allowed to cool down to room temperature, filtered, and washed with methanol (2 × 20 mL) and ethyl acetate (2 × 20 mL). After removal of the solvent, the crude product was purified by column chromatography over silica gel (eluent: petroleum ether: trichloromethane =1: 2) to give BT-CAR2 as a black solid. Further purification can be simply performed via recrystallization in methanol. (95 mg, yield: 85.6 %) ^{1}H NMR (400 MHz, Chloroform-d) δ: 8.23 (s, 1H), 7.82 (s, 1H), 7.75 (d, J = 4.1 Hz, 1H), 7.52 (d, J = 2.4 Hz, 2H), 7.33 (d, J = 4.0 Hz, 1H), 7.25 (s, 2H), 7.22 (d, J = 4.1 Hz, 1H), 7.18 (d, J = 4.1 Hz, 1H), 7.10 (d, J = 2.8 Hz, 2H), 7.00 (d, J = 7.1 Hz, 2H), 4.24 – 4.14 (m, 4H), 2.94 – 2.72 (m, 12H), 1.79 (p, J = 6.2 Hz, 2H), 1.74 – 1.63 (m, 9H), 1.52 – 1.24 (m, 53H), 1.04 – 0.87 (m, 30H). ^{13}C NMR (101 MHz, Chloroform-d) δ: 138.60, 135.49, 128.03, 122.88, 68.79, 40.88, 38.80, 32.54, 32.23, 31.72, 31.67, 30.33, 30.23, 29.89, 29.74, 29.32, 28.93, 28.85, 25.95, 23.77, 23.09, 22.96, 22.68, 22.65, 22.61, 14.24, 14.15, 14.12, 14.06, 12.30, 11.03, 10.95.

Synthesis of Compound BT-CAR4:

The synthesis of BT-CAR4 is similar to that of BT-CAR2. **4** (100 mg, 0.06 mmol) was used to get BT-CAR4 as a black solid (100 mg, yield: 88.7%)

^{1}H NMR (400 MHz, Chloroform-d) δ: 8.23 (d, J = 2.5 Hz, 1H), 7.80 (d, J = 4.0 Hz, 1H), 7.74 (d, J = 4.0 Hz, 1H), 7.50 (t, J = 2.6 Hz, 2H), 7.31 (d, J = 4.0 Hz, 1H), 7.21 (d, J = 3.9 Hz, 1H), 7.16 (d, J = 4.1 Hz, 1H), 7.08 (d, J = 4.2 Hz, 2H), 6.99 (dd, J = 8.8, 3.8 Hz, 2H), 4.21 (dd, J = 5.9, 2.3 Hz, 2H), 4.09 (t, J = 7.6 Hz, 2H), 2.96 – 2.85 (m, 4H), 2.78 (dq, J = 25.3, 8.0 Hz, 8H), 1.80 (p, J = 6.3 Hz, 2H), 1.75 – 1.62 (m, 11H), 1.53 – 1.23 (m, 52H), 1.04 – 0.86 (m, 33H). ^{13}C NMR (101 MHz, Chloroform-d) δ: 163.22, 146.25, 142.94, 138.58, 137.88, 136.26, 135.50,

130.94, 128.66, 128.04, 124.92, 122.88, 122.35, 68.79, 44.64, 40.88, 38.80, 32.55, 32.23, 31.72, 31.68, 30.31, 30.23, 29.91, 29.76, 29.33, 29.27, 29.06, 28.93, 28.85, 25.95, 23.77, 23.09, 22.97, 22.69, 22.64, 22.61, 20.10, 14.24, 14.15, 14.12, 14.11, 14.06, 13.70, 11.03, 10.96.

Synthesis of Compound BT-CAR6:

The synthesis of BT-CAR6 is similar to that of BT-CAR2. **4** (100 mg, 0.06 mmol) was used to get BT-CAR6 as a black solid (98.8 mg, yield: 86.3%)

^{1}H NMR (400 MHz, Chloroform-d) δ : 8.23 (s, 1H), 7.81 (s, 1H), 7.75 (d, J = 4.2 Hz, 1H), 7.52 (d, J = 3.0 Hz, 2H), 7.33 (d, J = 4.0 Hz, 1H), 7.25 (s, 2H), 7.22 (d, J = 4.1 Hz, 1H), 7.18 (d, J = 4.0 Hz, 1H), 7.10 (d, J = 3.2 Hz, 2H), 7.00 (d, J = 7.9 Hz, 2H), 4.21 (dd, J = 5.8, 2.3 Hz, 2H), 4.12 – 4.05 (m, 2H), 2.93 – 2.71 (m, 12H), 1.79 (p, J = 6.4 Hz, 2H), 1.74 – 1.63 (m, 11H), 1.51 – 1.24 (m, 56H), 1.04 – 0.87 (m, 33H). ^{13}C NMR (101 MHz, Chloroform-d) δ: 138.61, 135.49, 134.63, 128.69, 128.03, 122.88, 40.88, 38.80, 32.54, 32.22, 31.72, 31.67, 31.35, 30.32, 30.23, 30.01, 29.74, 29.35, 29.31, 29.26, 28.93, 28.85, 26.94, 26.46, 25.94, 23.77, 23.08, 22.96, 22.68, 22.61, 22.52, 14.23, 14.15, 14.11, 14.07, 14.02, 11.03, 10.95.

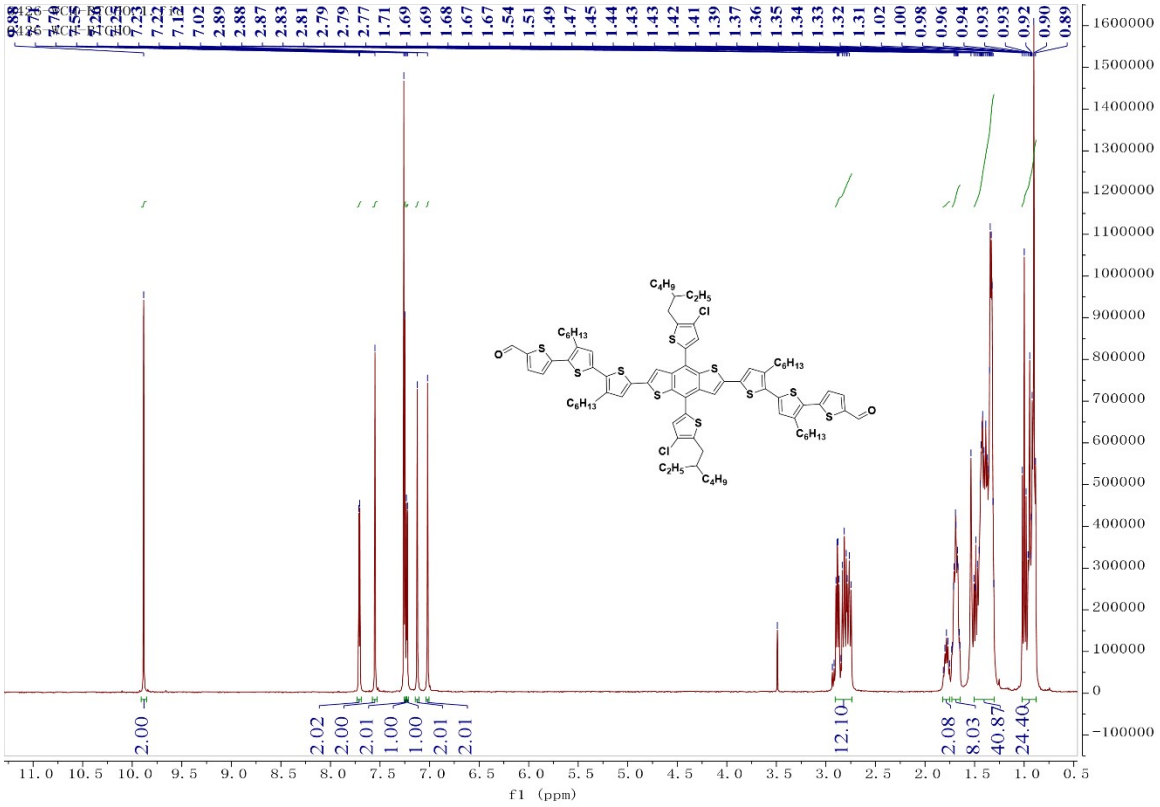

Fig. S1 ^{1}H-NMR spectrum of compound 3.

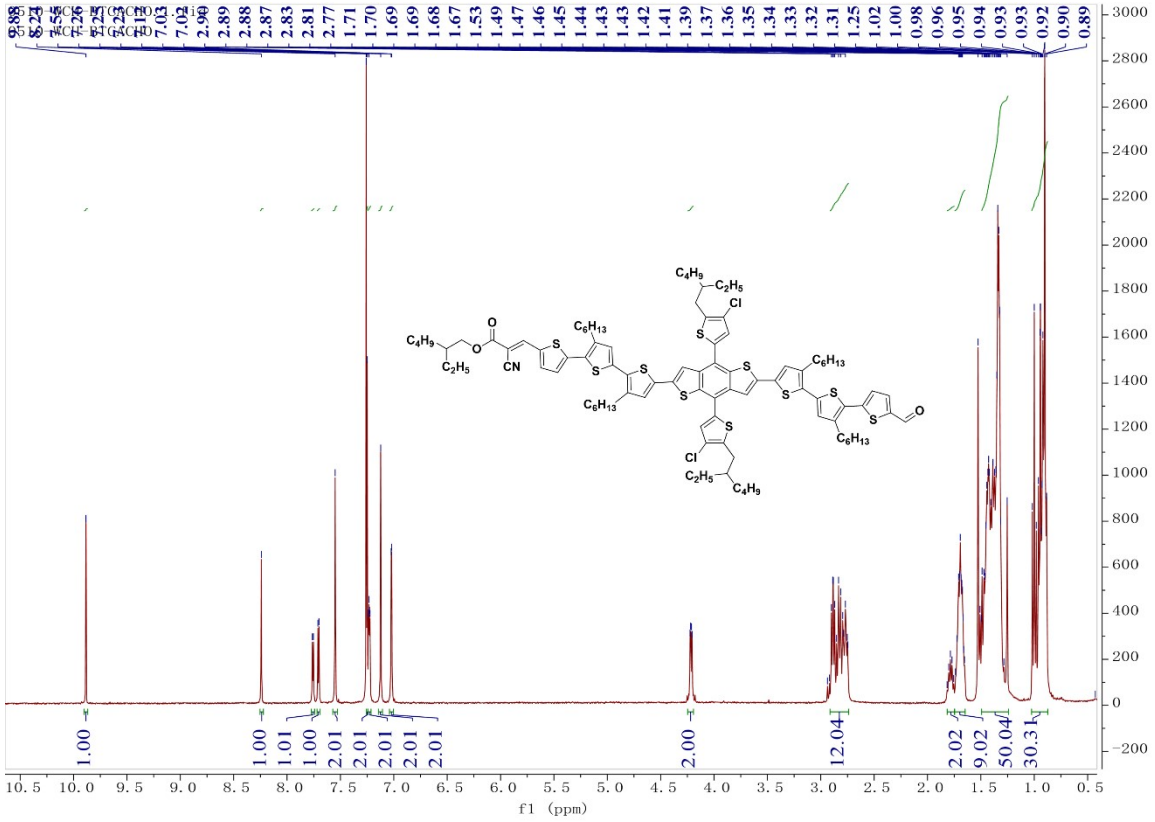

Fig. S2 ^{1}H-NMR spectrum of compound 4.

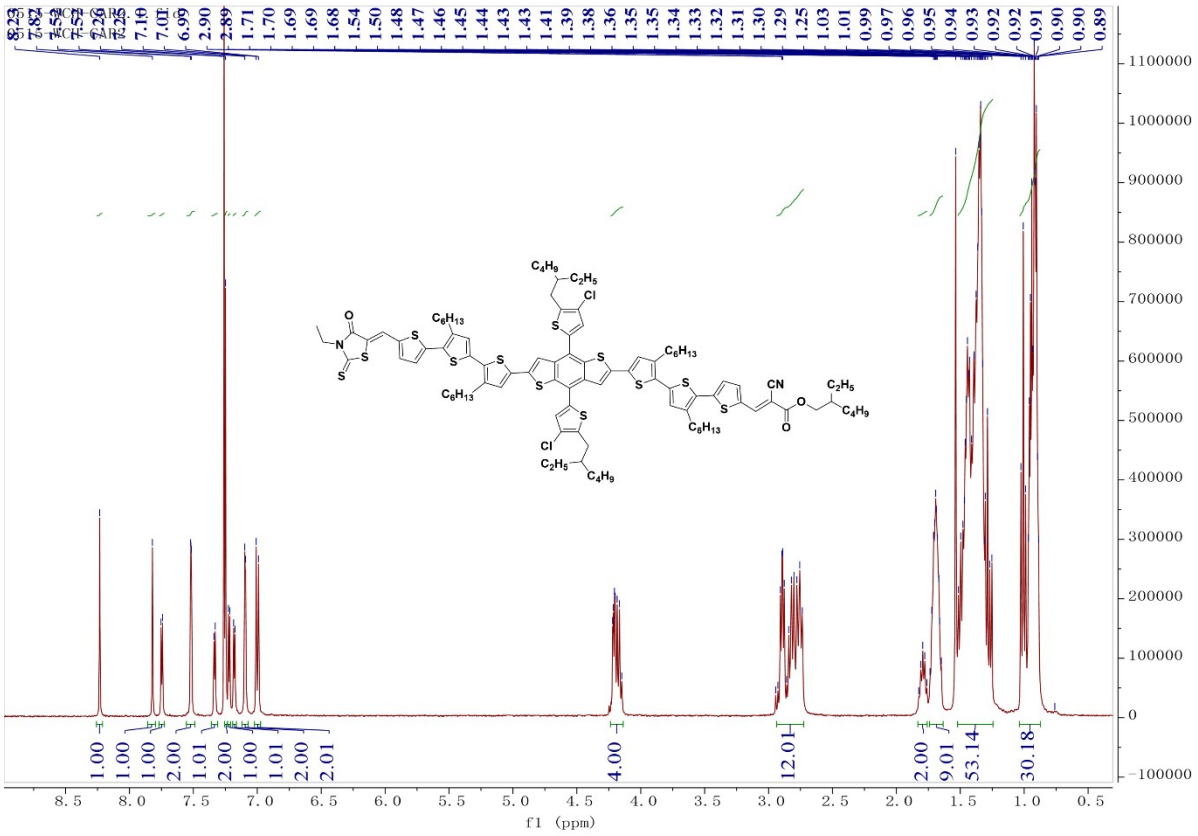

Fig. S3 ^{1}H-NMR spectrum of BT-CAR2.

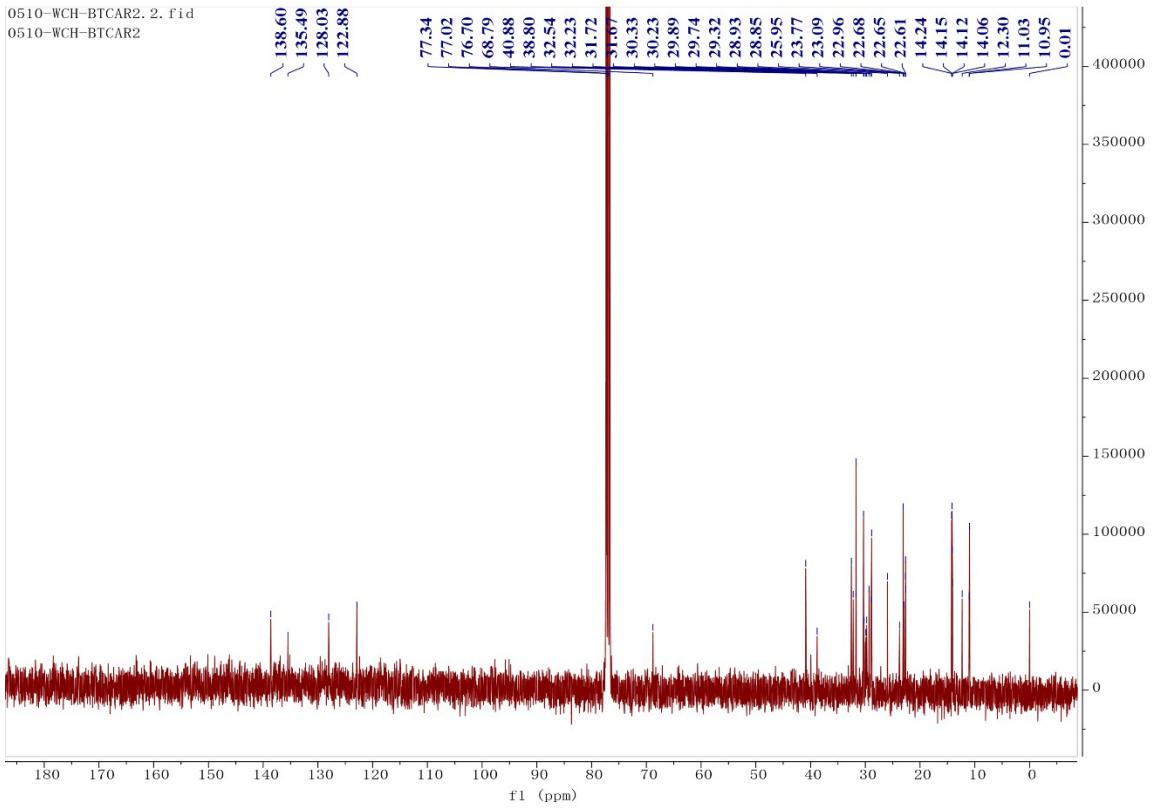

Fig. S4 ^{13}C-NMR spectrum of BT-CAR2.

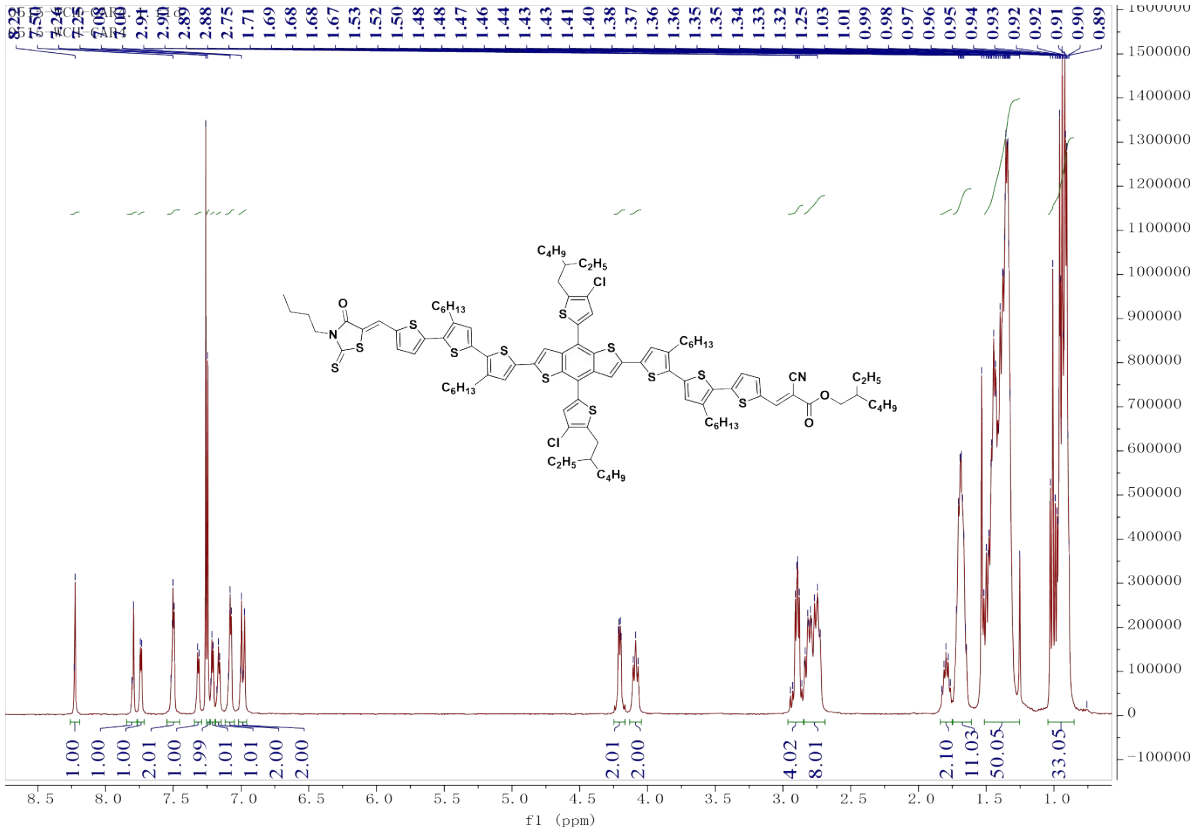

Fig. S5 ^{1}H-NMR spectrum of BT-CAR4.

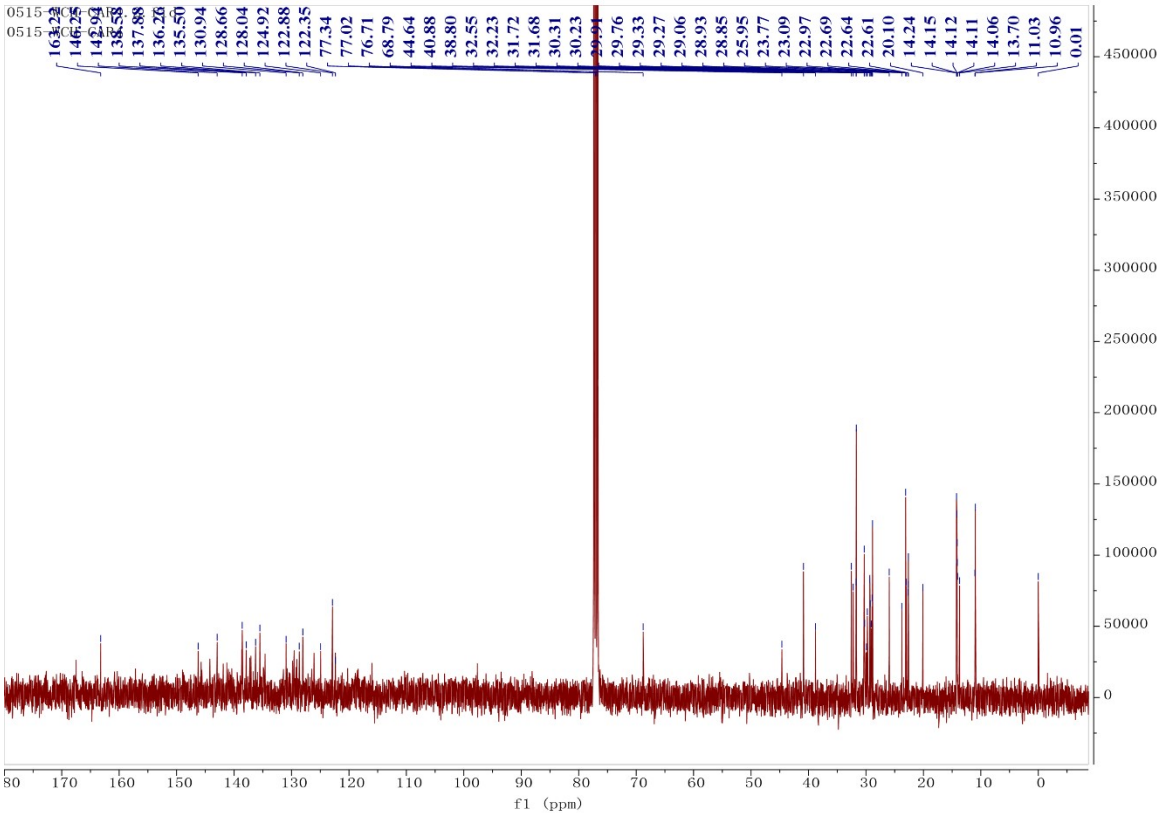

Fig. S6 ^{13}C-NMR spectrum of BT-CAR4.

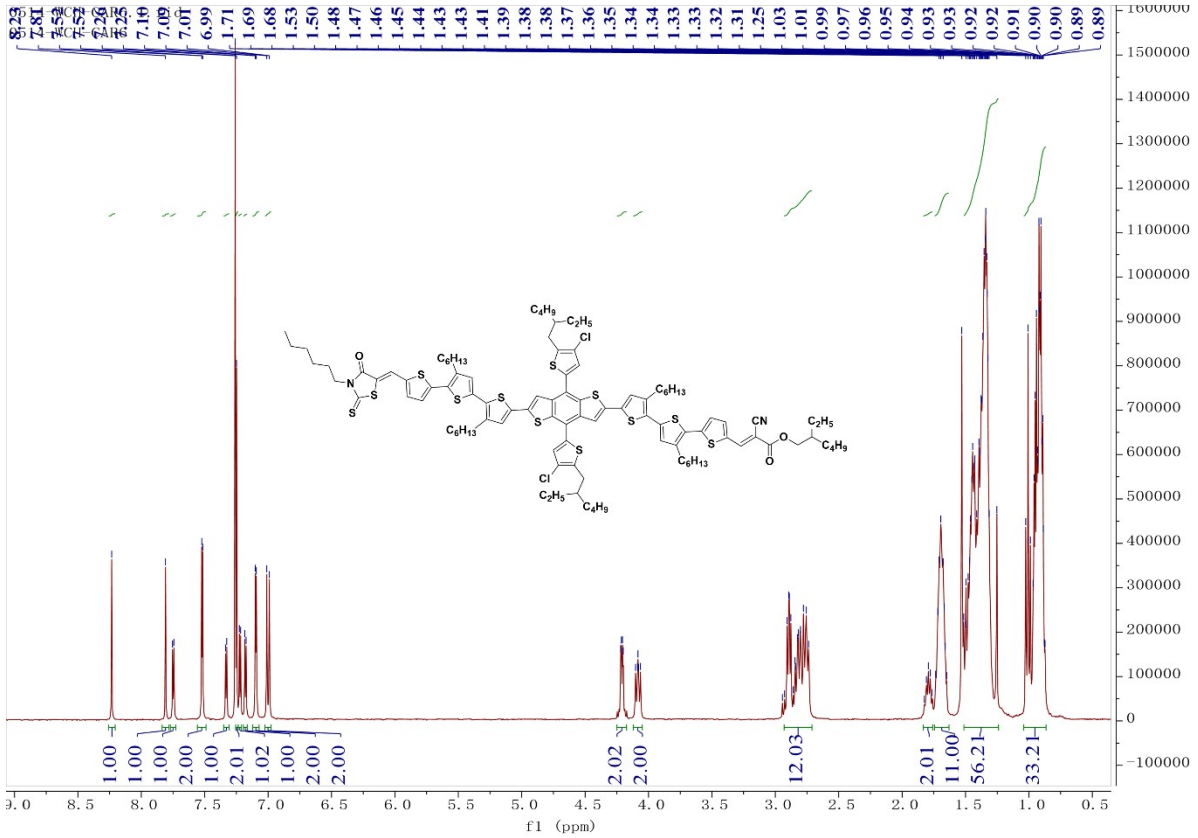

Fig. S7 ^{1}H-NMR spectrum of BT-CAR6.

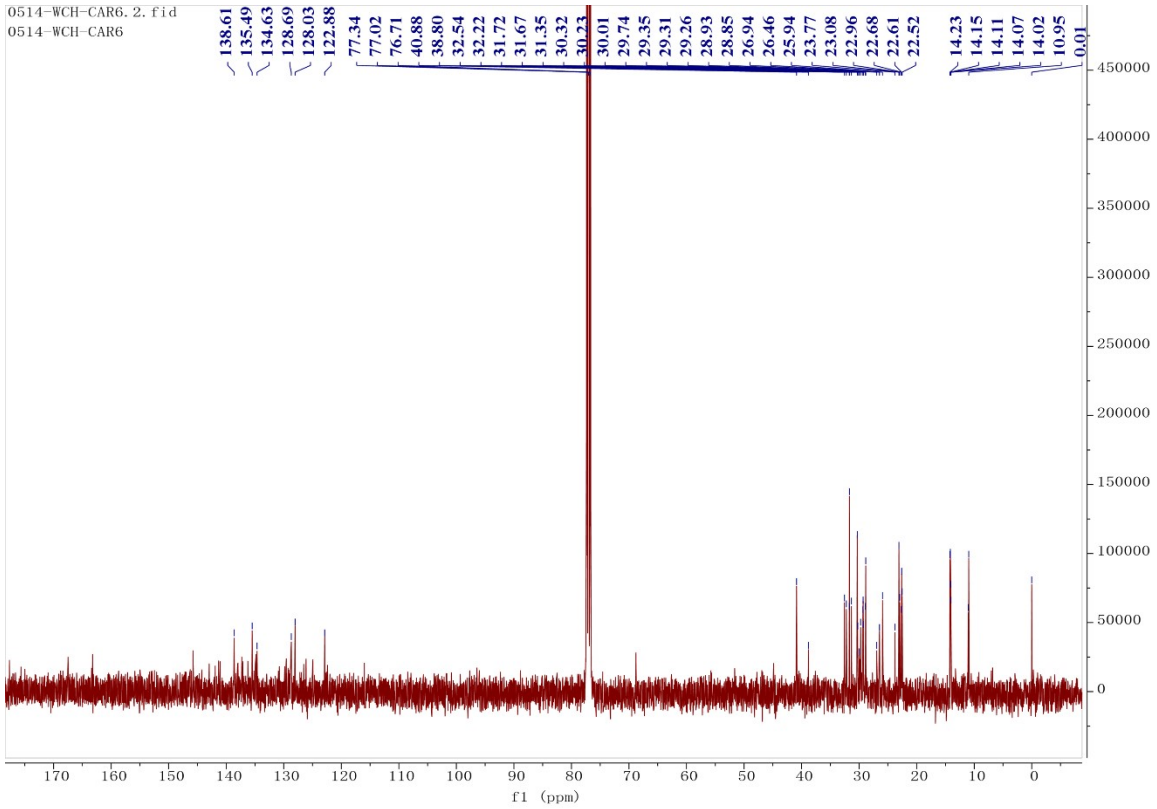

Fig. S8 ^{13}C-NMR spectrum of BT-CAR6.

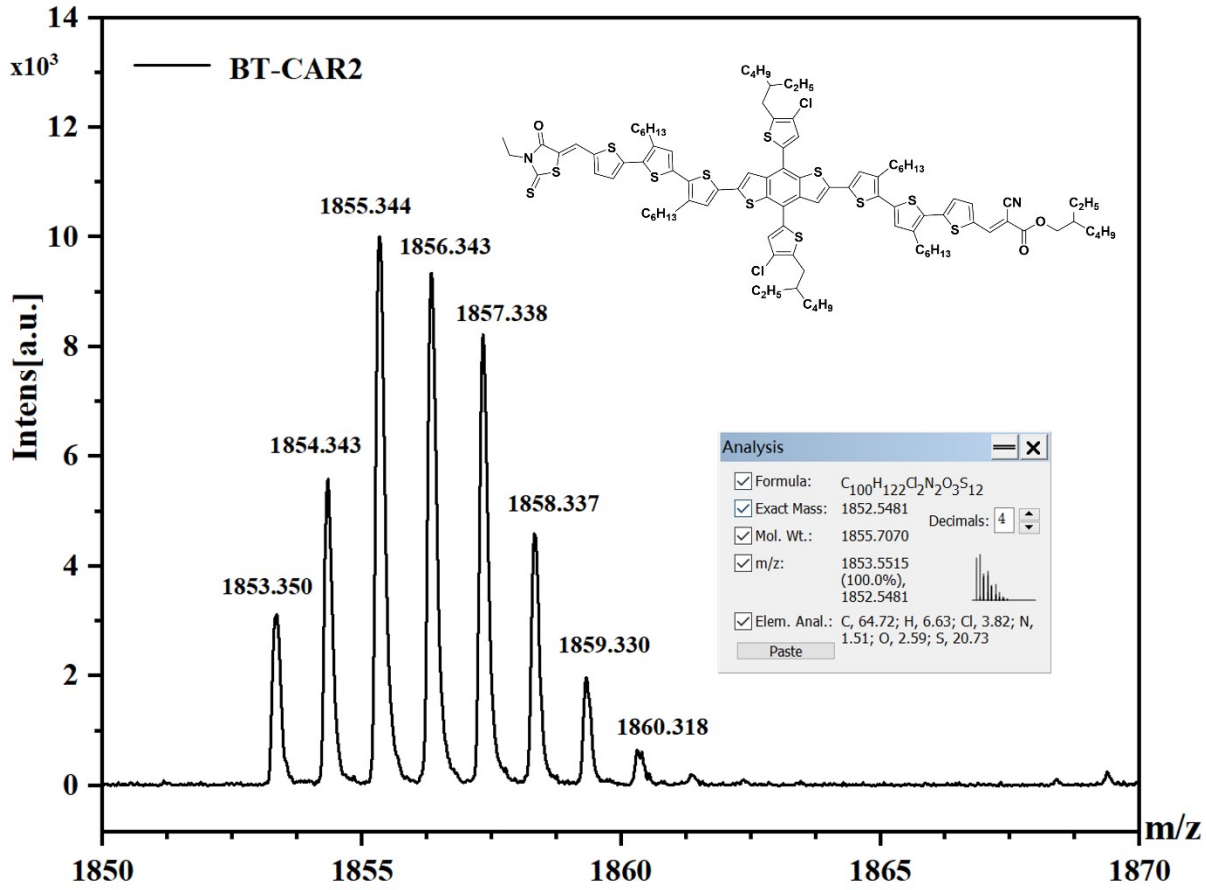

Fig. S9 MALDI-TOF mass spectrum of BT-CAR2.

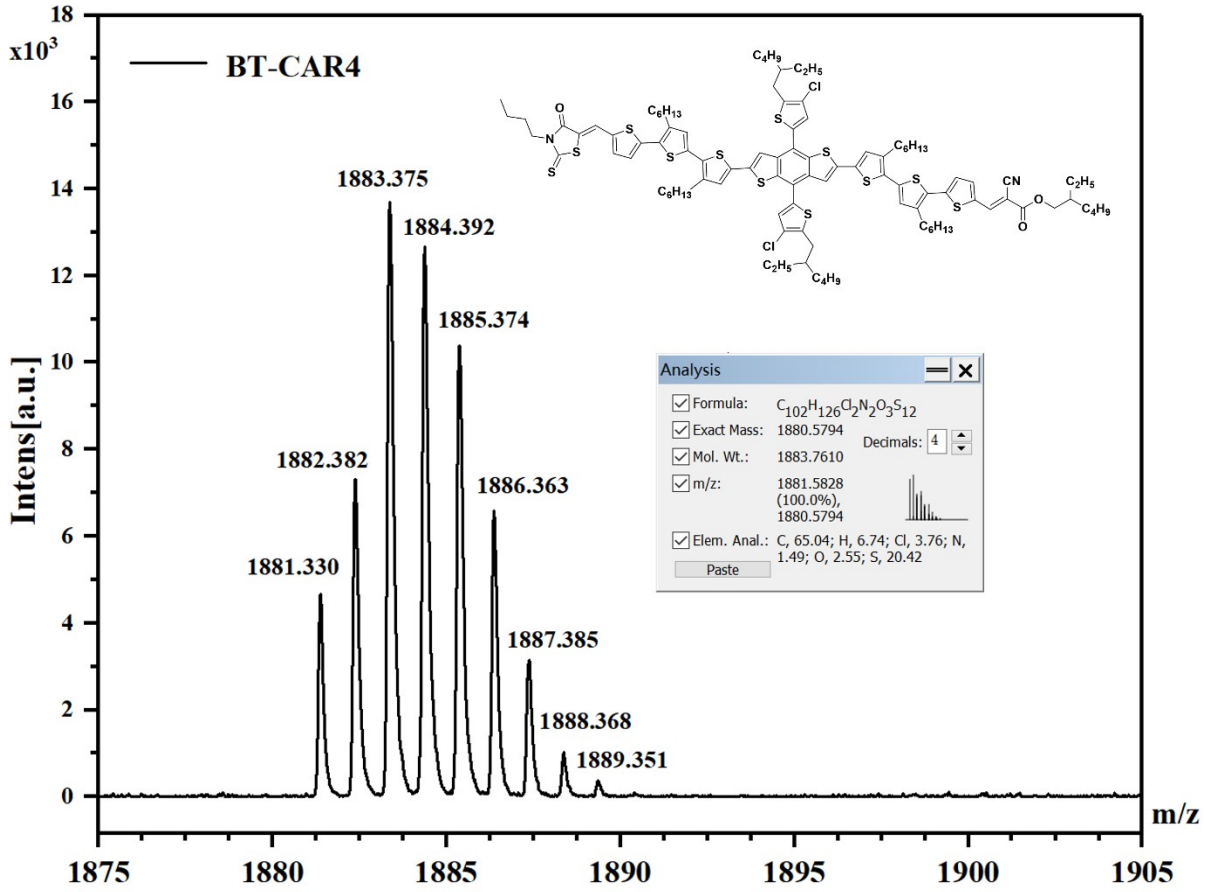

Fig. S10 MALDI-TOF mass spectrum of BT-CAR4.

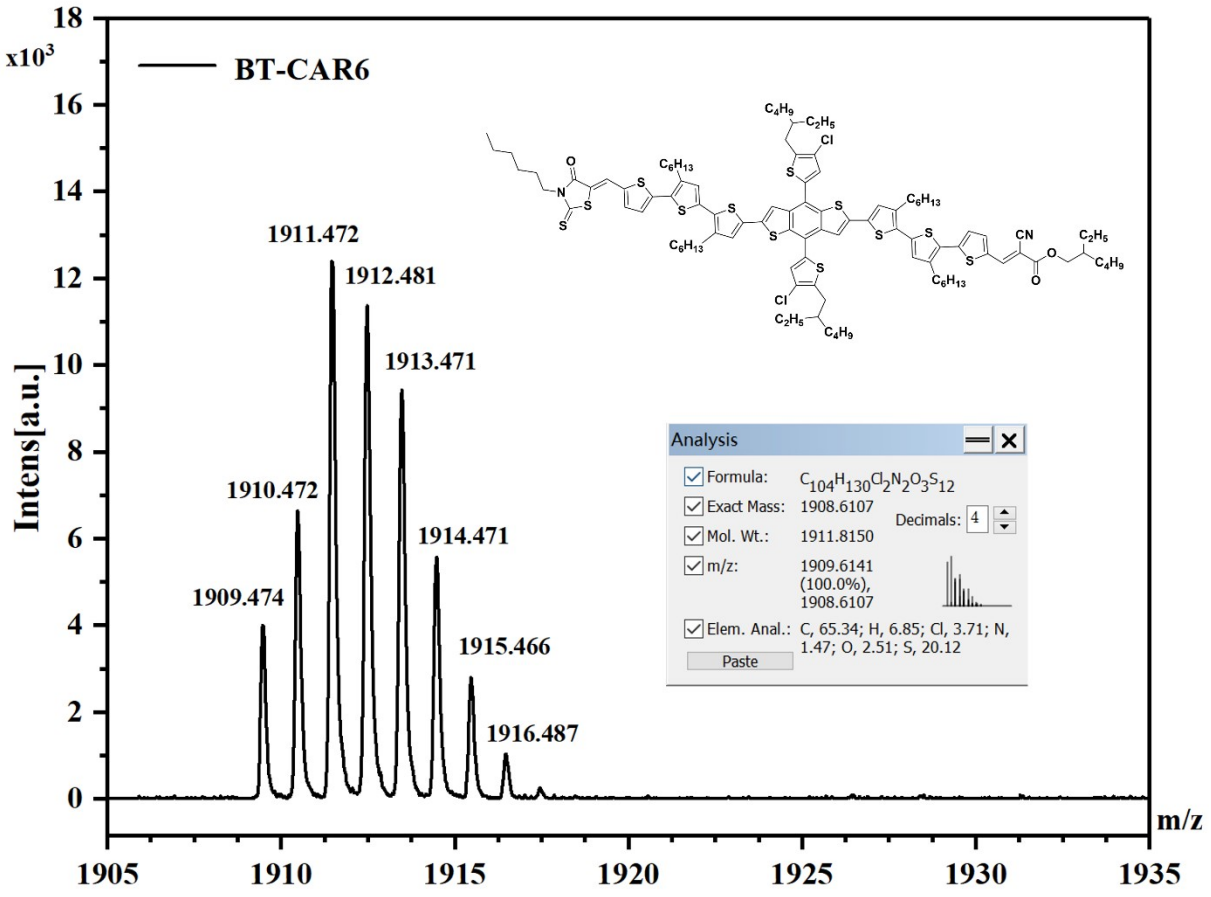

Fig. S11 MALDI-TOF mass spectrum of BT-CAR6.

Characterization

NMR Measurement：^{1}H-NMR and ^{13}C-NMR spectra were obtained on a Bruker Advance III 400 (400 MHz) nuclear magnetic resonance (NMR) spectroscope.

MALDI-TOF Measurement: Matrix-assisted laser desorption/ionization time-of-flight (MALDI-TOF) mass spectrum tests were carried out on a Walters Maldi Q-TOF Premier mass spectrometry.

TGA Measurement: Thermogravimetric analysis (TGA) was done on a Netzsch STA409PC TG/DSC Thermal Analyzer under N_2 atmosphere at a heating rate of 10℃/min.

DSC Measurement: Differential scanning calorimetry analysis (DSC) was done on a TA DSC Q100 Differential Scanning Calorimeter under N_2 atmosphere at a heating rate of 10℃/min.

Quantum Chemical Calculation: Density functional theory (DFT) calculations were conducted at the B3LYP/6-31G(d) level to obtain the optimized molecular geometries and frontier molecular orbitals of the Donors. All alkyl substituents were replaced with methyl groups to save computational time.

UV-vis Measurement: UV-vis absorption spectra were recorded on a Shimadzu UV-1800 spectrophotometer.

CV Measurement: Cyclic voltammetry (CV) measurements were carried out on a CHI600A electrochemical workstation with Pt plate as the working electrode, Pt wire as the counter electrode, and standard calomel electrode (SCE) as the reference electrode anhydrous acetonitrile solution containing 0.1 mol/L tetrabutylammoniumhexafluorophosphate (Bu_4NPF_6) as the supporting electrolyte. All potentials were corrected against ferrocene/ferrocenium (Fc/Fc^+) whose absolute energy level is 4.8 eV below vacuum. The equation of $E_{LUMO/HOMO}$ = -e($E_{red/ox}$+4.41) (eV) was used to calculate the LUMO and HOMO levels (the redox potential of $Fc/Fc^+$is found to be 0.39 V).

Device fabrication: Organic solar cells were fabricated on glass substrates commercially pre-coated with a layer of ITO with the conventional structure of ITO/PEDOT:PSS/Donor:Acceptor/PDINN/Ag. Before fabrication, the substrates were cleaned

using detergent, deionized water, acetone, and isopropanol consecutively for 20 min in each step and dried up. Then the substrates were treated in an ultraviolet ozone generator for 20 min before being spin-coated at 4500 rpm with a layer of 20 nm thick PEDOT:PSS (Baytron P AI4083). After baking the PEDOT:PSS layer in air at 150 ℃for 15 min, they were transferred to a glovebox. The optimized active layers were spin-coated from the corresponding chloroform solutions (20 mg/mL, BT-CAR2: Y6 = 1: 1 (by wt.); BT-CAR4: Y6 = 1: 1 (by wt.); BT-CAR6: Y6 = 1: 1 (by wt.). Then the active layers were solvent vapor annealed with chlorobenzene in a 60 mm diameter dish for 150 s. Then, the PDINN film was deposited as the cathode buffer layer by the spin-coating of a solution of 1 mg/mL PDINN in methanol at 3500 rpm. Finally, the Ag (100 nm) electrode was deposited by thermal evaporation to complete the device with an active area of 6 mm^2.

***J-V* curves and EQE data:** The current density-voltage (*J-V*) curves of OSCs were performed on an Enlitech SSX50 solar simulator under the condition of AM 1.5 G illumination and the light intensity was calibrated by a standard Si solar cell at 100 mV cm^{-2}. The EQE data were measured by a Solar Cell Spectral Response Measurement System (RE-R, Enlitech). All the devices mentioned were tested by a shadow mask with an area of 0.0473 cm^2.

SCLC Mobility Measurement: Using the space-charge-limited current (SCLC) method to measure the charge carrier mobilities of the blend films. Hole-only devices were fabricated in a structure of ITO/PEDOT:PSS/Donor:Acceptor/MoO_3/Ag, and electron-only devices were fabricated in a structure of ITO/ZnO/Donor:Acceptor/PDINN/Ag. The device characteristics were extracted by modeling the dark current under forward bias using the SCLC expression described by the Mott-Gurney law:

$$J = \frac{9}{8}\varepsilon_r\varepsilon_0\mu\frac{V^2}{L^3}$$

Here, $\varepsilon_r \approx 3$ is the average dielectric constant of the blend film, ε_0 is the permittivity of the free space, μ is the carrier mobility, L is the thickness of the film (~100 nm), and V is the applied voltage.

Transient Absorption Measurement: For femtosecond transient absorption spectroscopy, the fundamental output from Yb:KGW laser (1030 nm, 220 fs Gaussian fit, 100 kHz, Light

Conversion Ltd) was separated to two light beam. One was introduced to NOPA (ORPHEUS-N, Light Conversion Ltd) to produce a certain wavelength for pump beam (here we use 820 nm, <10 μJ/cm^2), the other was focused onto a YAG plate to generate white light continuum as probe beam. The pump and probe overlapped on the sample at a small angle less than 10°. The transmitted probe light from sample was collected by a linear CCD array. Then we obtained transient differential transmission signals by equation shown below:

$$\frac{\Delta T}{T} = \frac{T_{pump-on} - T_{pump-off}}{T_{pump-off}}$$

AFM Measurement: Topographic images of the films were obtained on a VeecoMultiMode atomic force microscopy (AFM) in the tapping mode using an etched silicon cantilever at a nominal load of ~2 nN, and the scanning rate for a 10 μm × 10 μm image size was 1.5 Hz and for a 1 μm × 1 μm image size was 1.0 Hz.

Surface Tension Measurement: Contact angle test was conducted on a LAUDA Scientific LSA series video optical contact angle tension measuring instrument. The surface tension values of films are calculated by the Wu method[1]. The Flory-Huggins interaction parameters are deduced from: $\chi^{D-A} = \kappa (\sqrt{\gamma D} - \sqrt{\gamma A})^2$

GIWAXS measurement: GIWAXS measurements were performed in a Xeuss 3.0 SAXS/WAXS system with a wavelength of λ = 1.341 Å at Vacuum Interconnected Nanotech Workstation (Nano-X).

Time-of-Flight Secondary Ion Mass Spectrometry (TOF-SIMS) Measurement：Cs+ was used as the sputter source with a 500 eV energy and 20 nA current. The typical sputter area was 200 μm by 200 μm. The "Normalized Depth" data is derived by normalizing the actual sputtering times of the samples against the total sputtering time that reaches the bottom of the substrate.

Supporting Figures

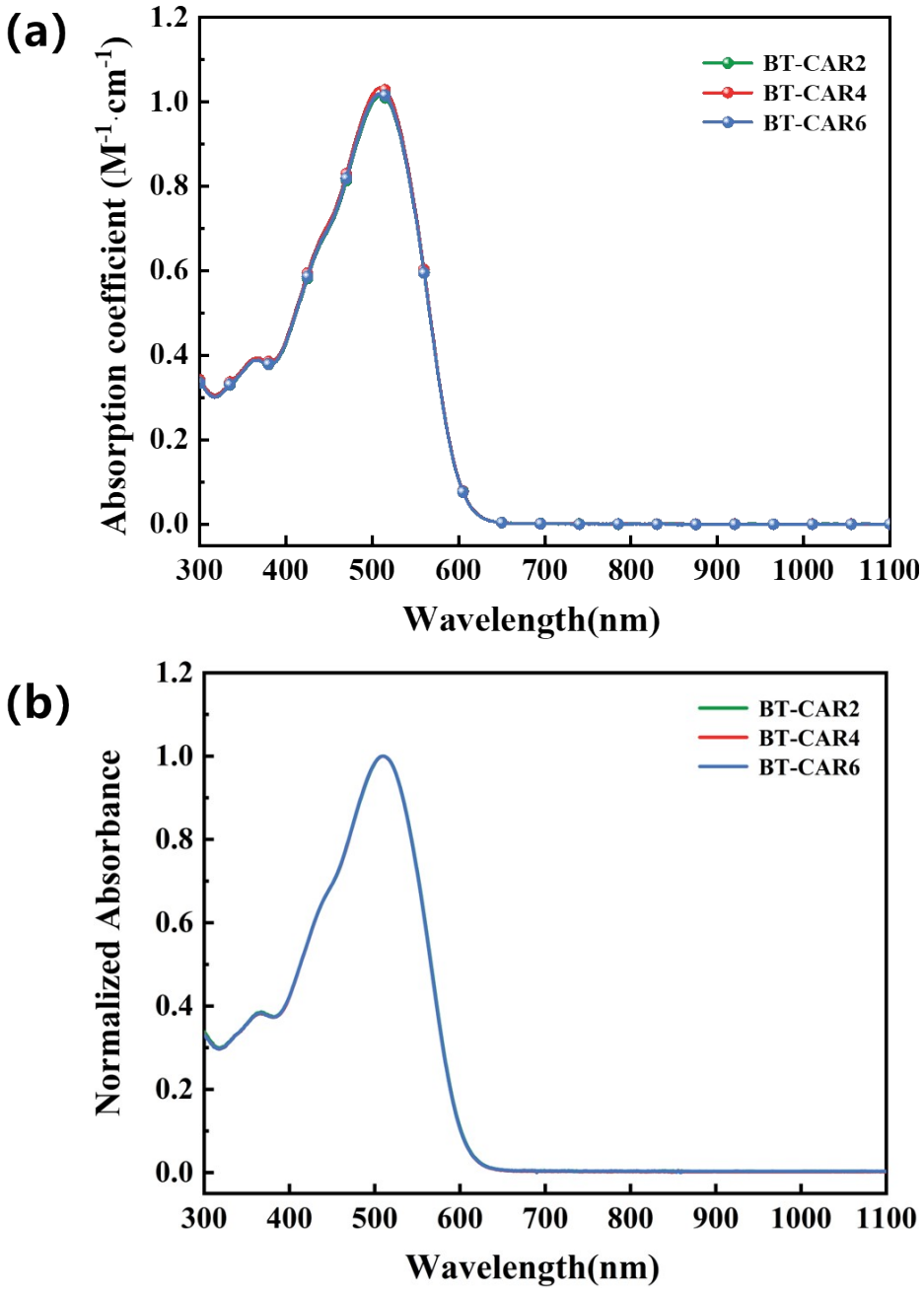

Fig. S12 (a) UV-vis spectra of BT-CAR2, BT-CAR4, and BT-CAR6 in dilute chloroform solutions ($1x10^{-5}$ $mol \cdot L^{-1}$). (b) Normalized UV-vis spectra of BT-CAR2, BT-CAR4, and BT-CAR6 in chloroform solutions.

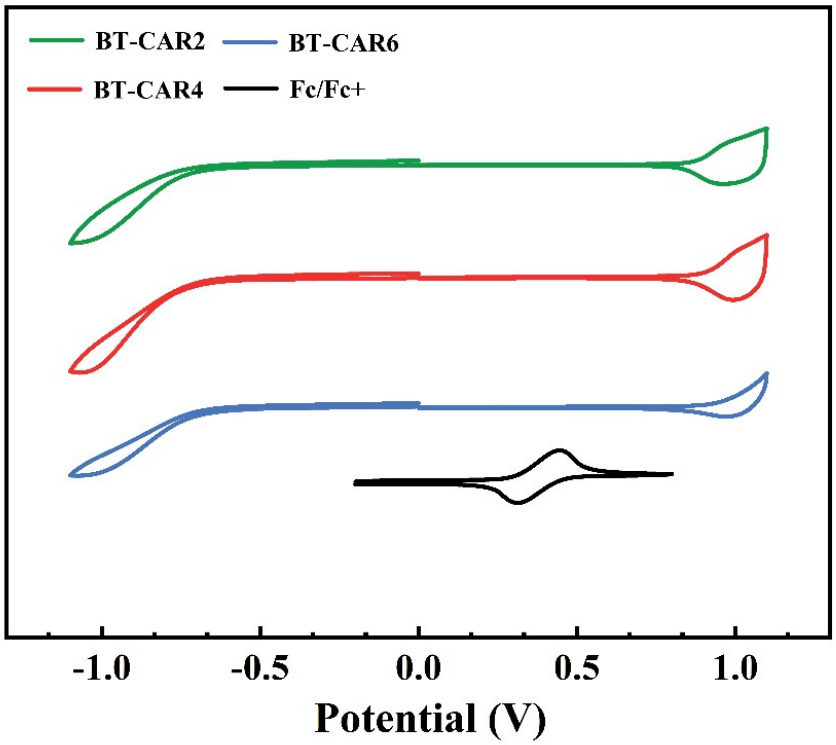

Fig. S13 Cyclic voltammograms of BT-CAR2, BT-CAR4, BT-CAR6, and Fc/Fc^{+} in acetonitrile solutions.

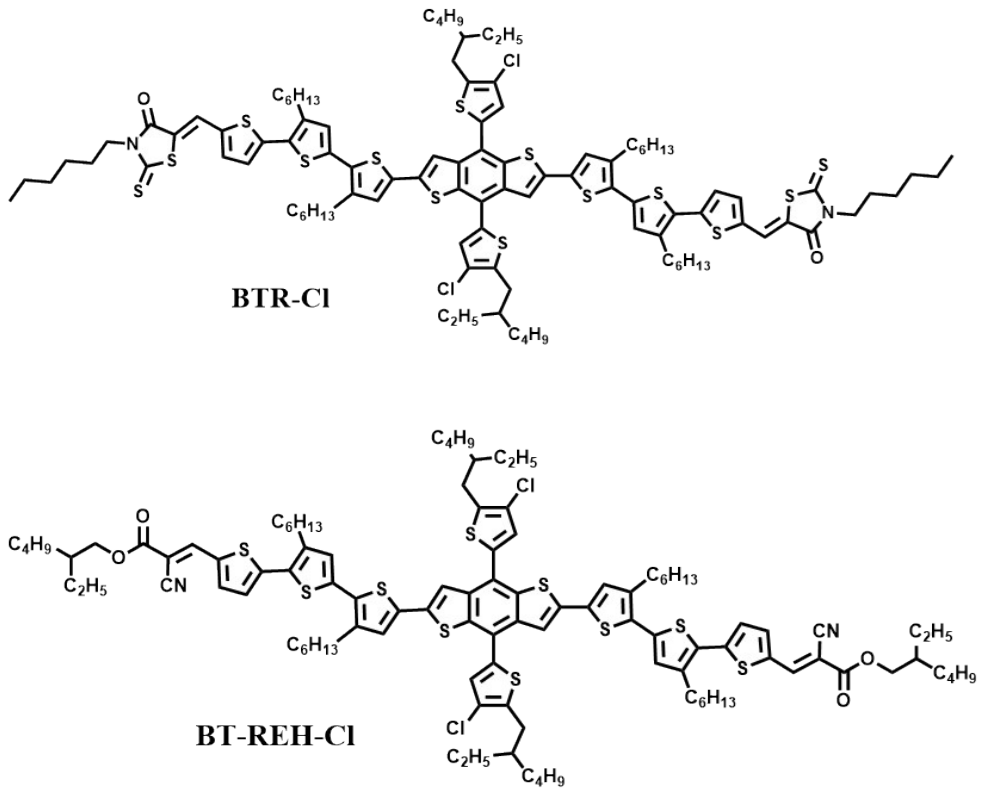

Fig. S14 The chemical structure of BTR-Cl and BT-REH-Cl.

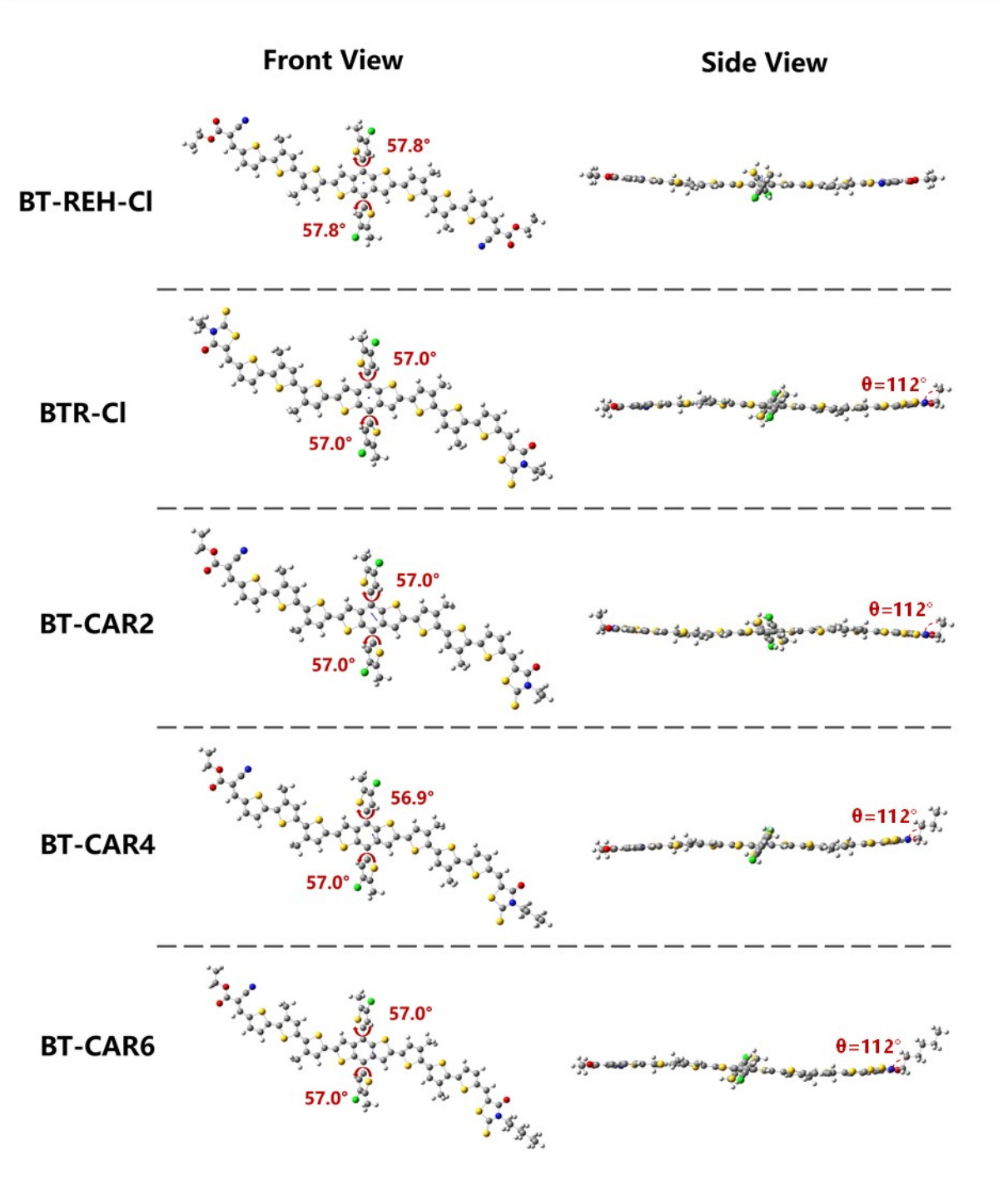

Fig. S15 Chemical geometry of the molecular models.

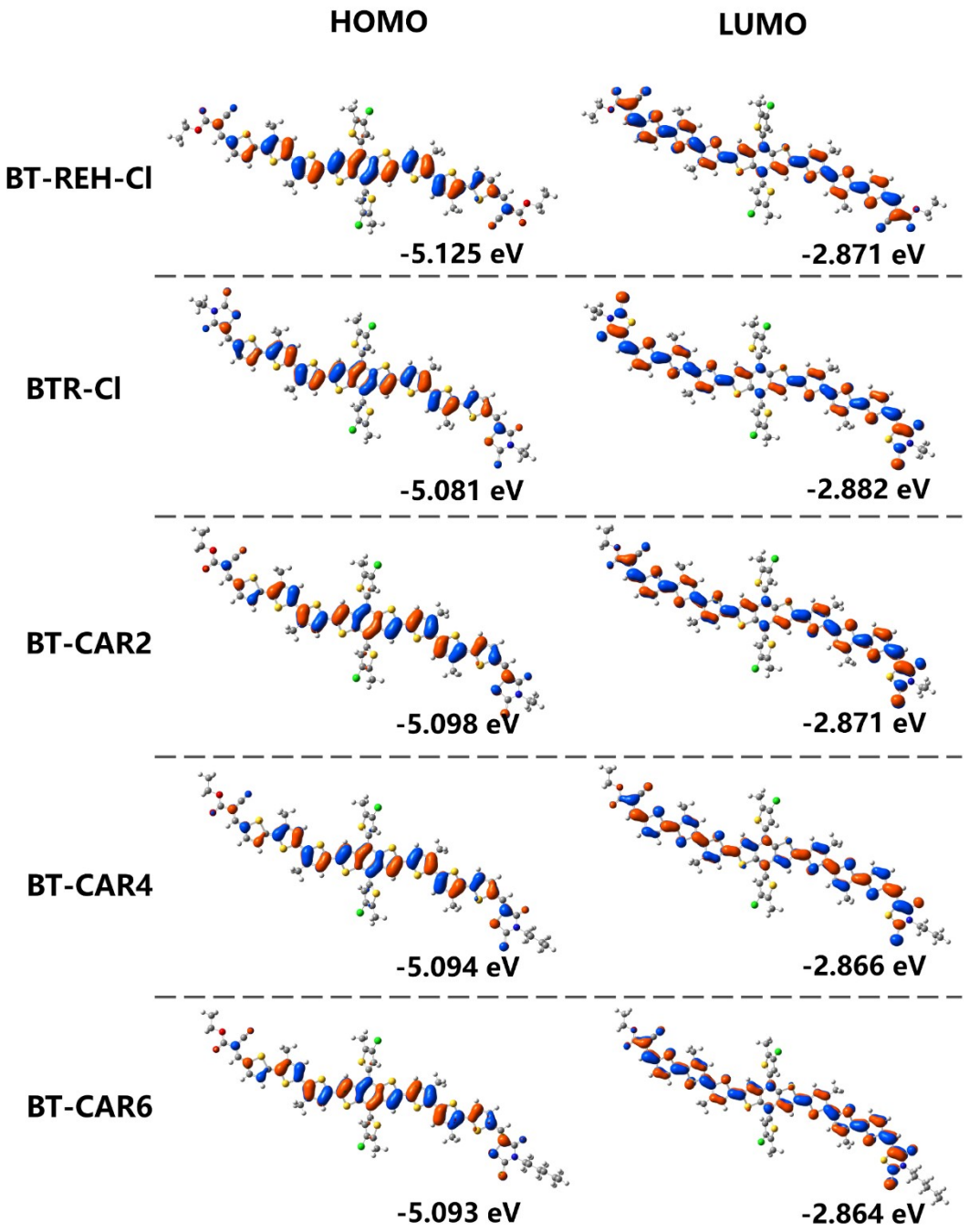

Fig. S16 HOMO and LUMO energy levels of the small molecular donors estimated by DFT calculation.

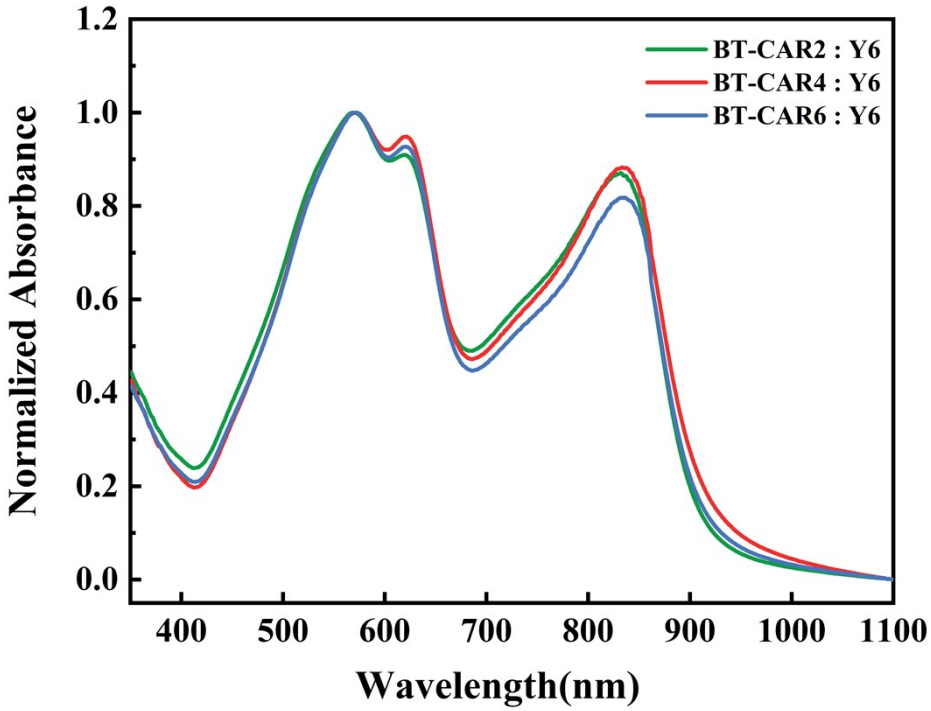

Fig. S17 Normalized UV-vis spectra of BT-CAR2:Y6, BT-CAR4:Y6, and BT-CAR6:Y6 blend films.

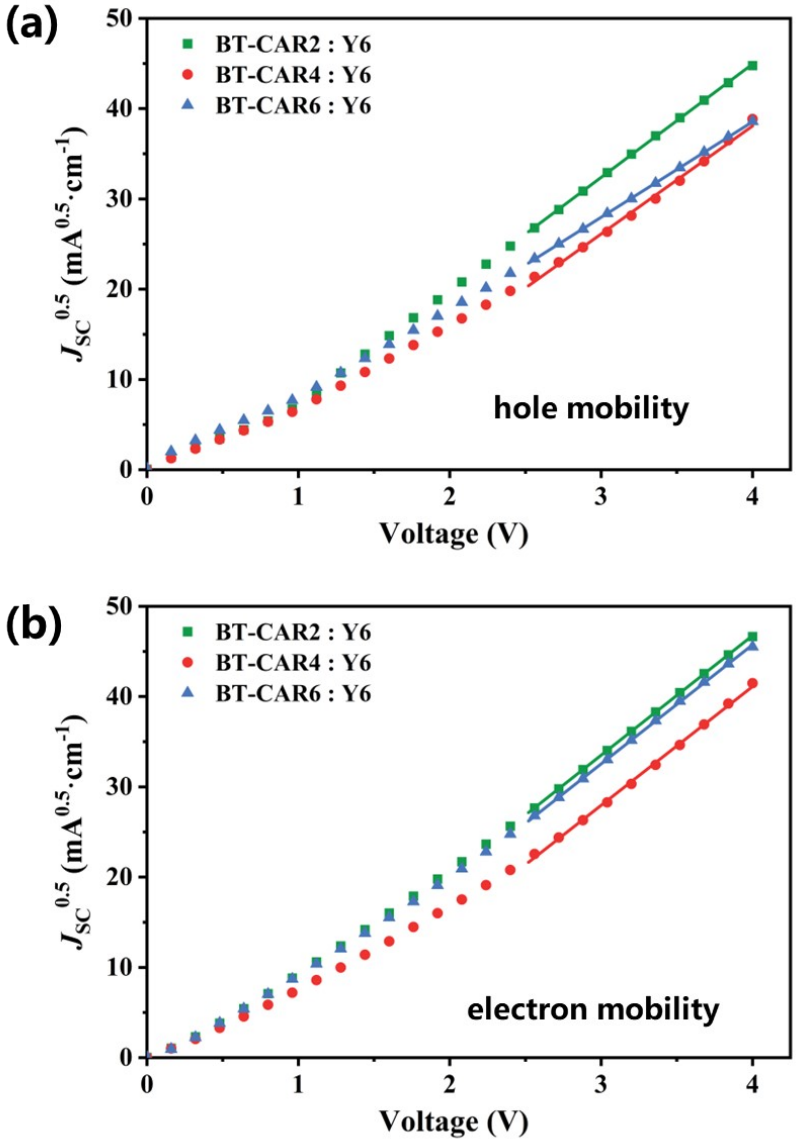

Fig. S18 $J^{0.5}$-V curves of (a) hole-only devices and (b) electron-only devices.

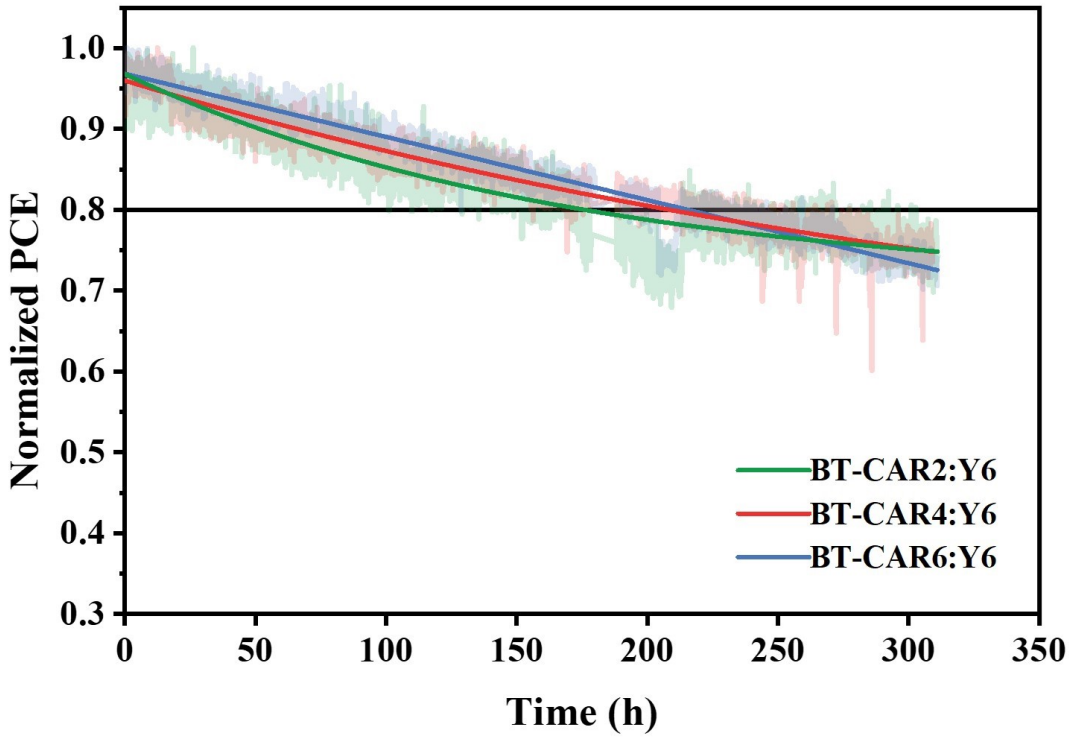

Fig. S19 The photo-stabilities of the three ASM-OSCs were tracked under maximum power point (MPP) conditions using 1-sun illumination.

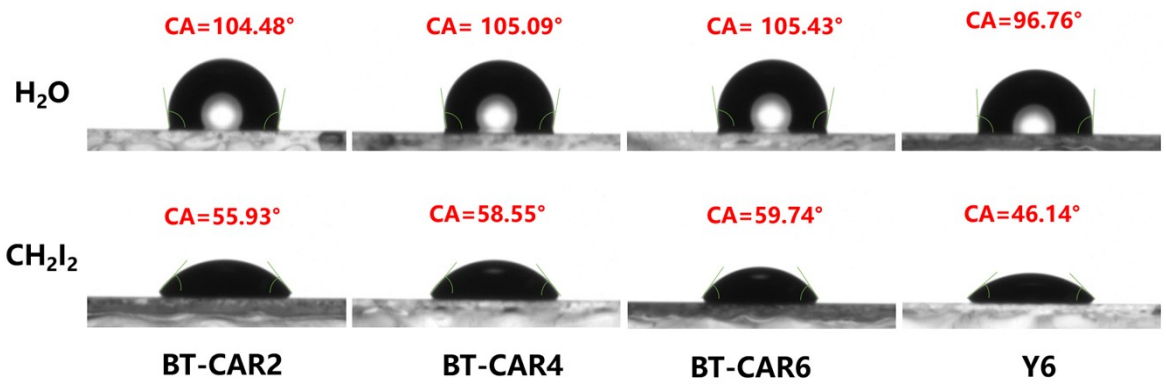

Fig. S20 The contact angle images of BT-CAR2, BT-CAR4, BT-CAR6, and Y6 neat films. Ultra-pure water and diiodomethane are used as wetting liquid.

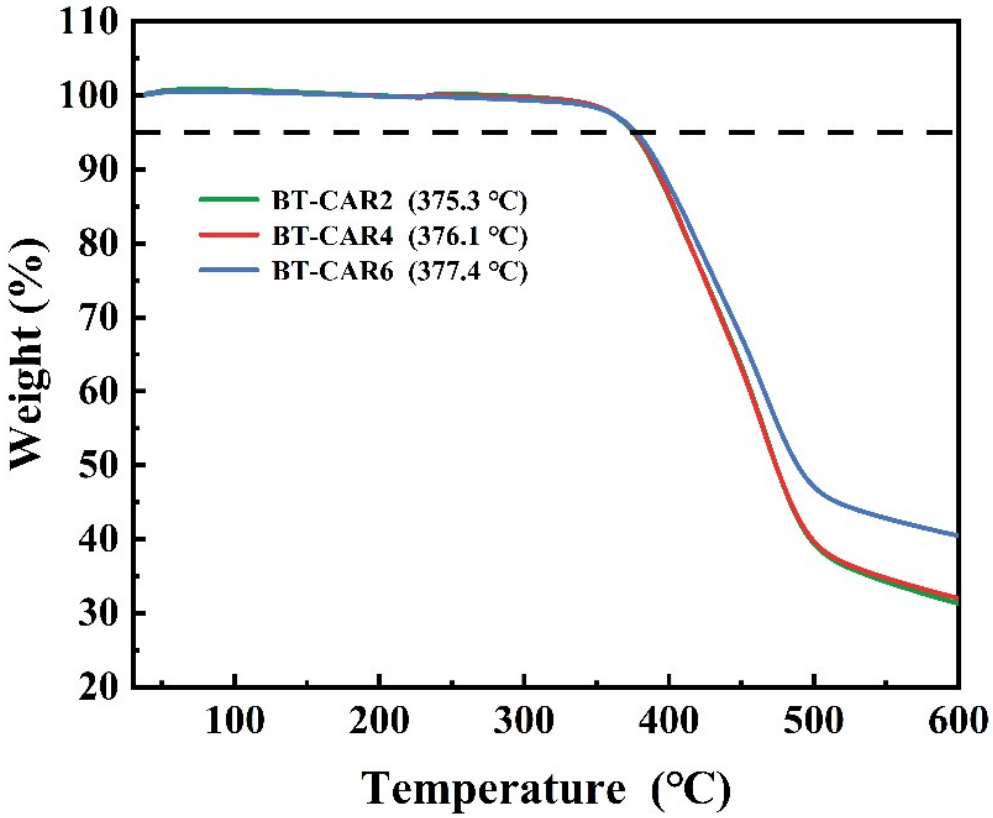

Fig. S21 TGA curves of BT-CAR2, BT-CAR4, and BT-CAR6.

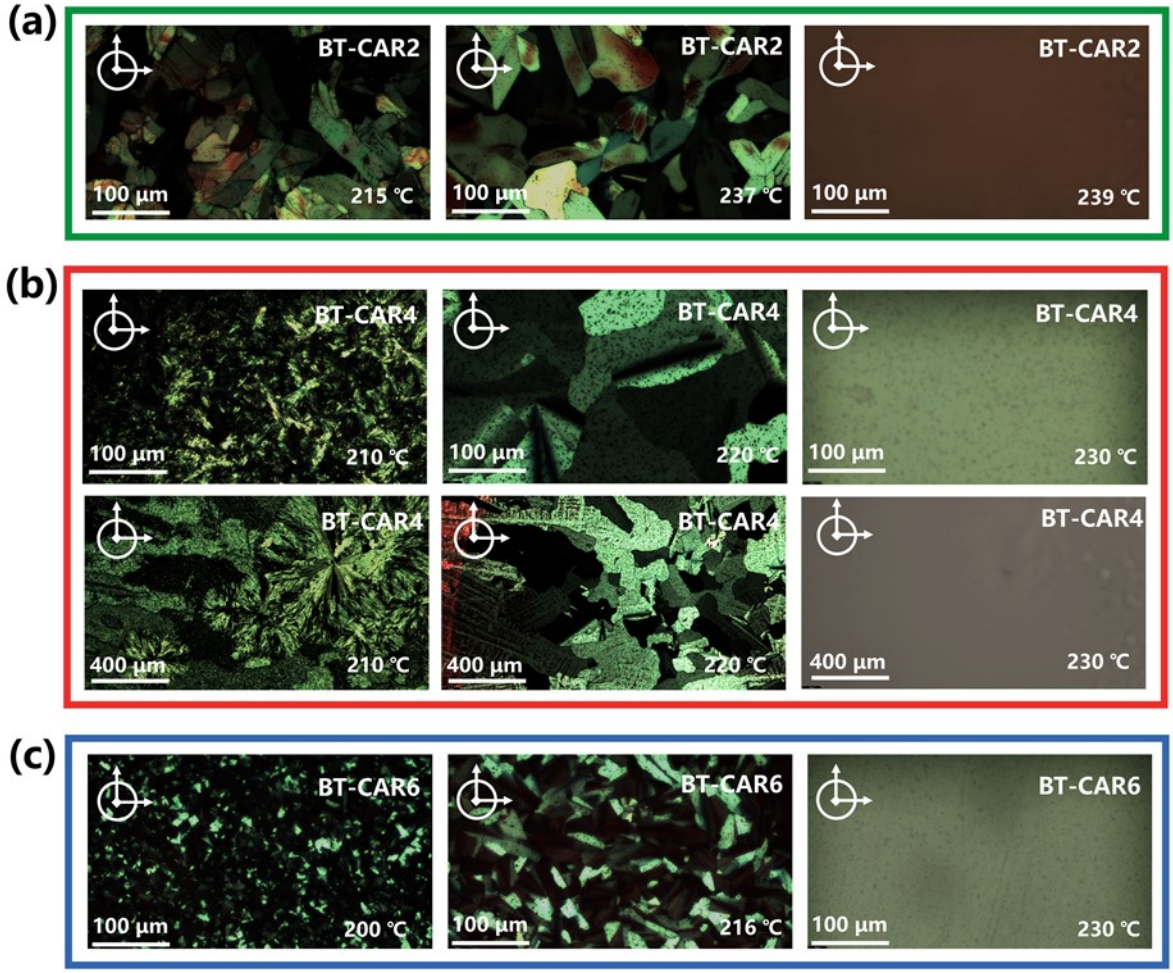

Fig. S22 POM images of (a) BT-CAR2, (b) BT-CAR4, and (c) BT-CAR6 neat films taken at different temperatures. The angle of the polarizer and the analyzer is 90°.

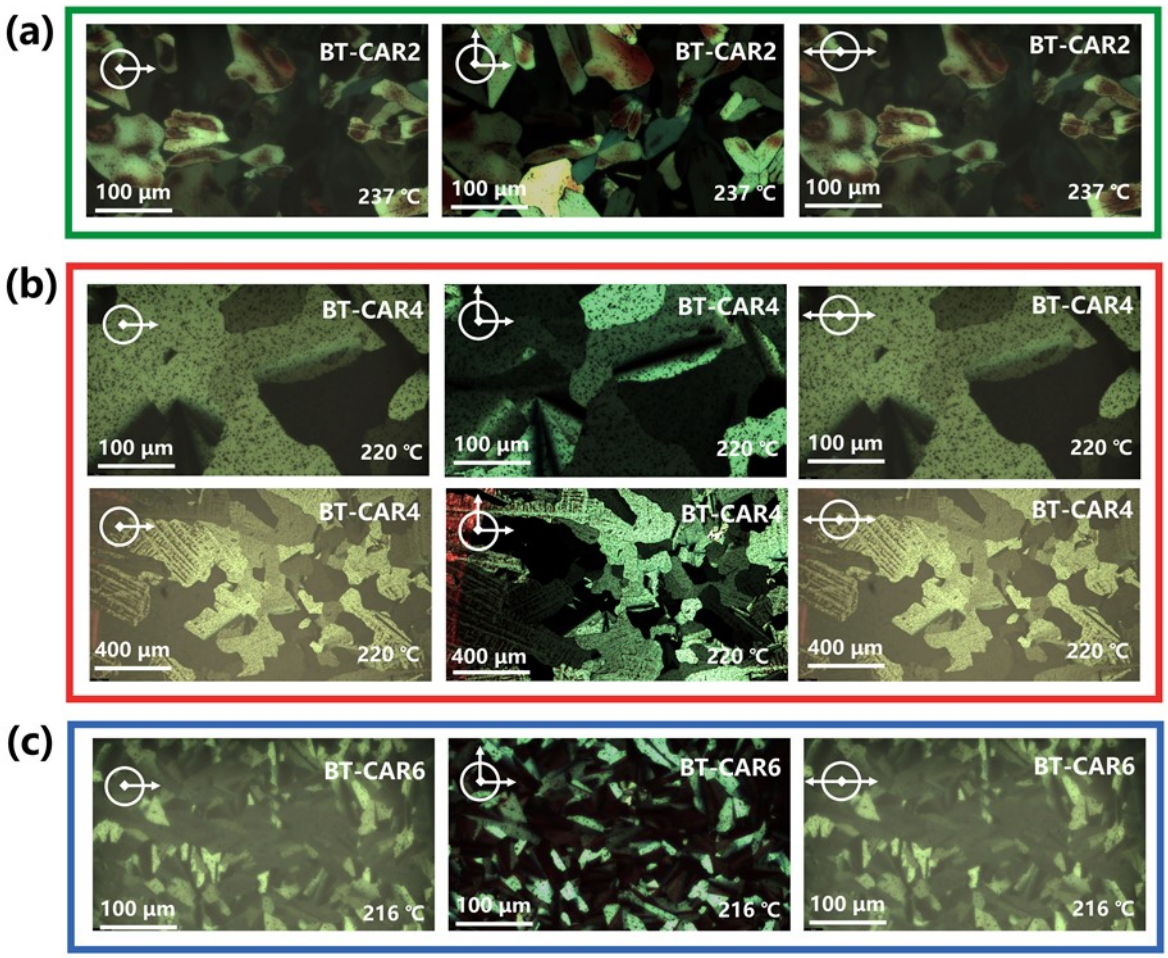

Fig. S23 POM images of (a) BT-CAR2, (b) BT-CAR4, and (c) BT-CAR6 pure films taken at a stage temperature of 237℃, 220℃, and 216℃, respectively. The pure films are sandwiched between two glass slides and observed with different polarized light angle.

Supporting Tables

Table S1 Summary of the GIWAXS parameters for the films.

Compound	Peak	Position / Å^{-1}	D-spacing / Å	FWHM / Å^{-1}	Coherence length / Å
BT-CAR2	(100) OOP	0.314	20.00	0.048	118.9
	(010) IP	1.737	3.62	0.297	19.2
BT-CAR4	(100) OOP	0.313	20.06	0.054	103.9
	(010) IP	1.757	3.57	0.313	17.9
BT-CAR6	(100) OOP	0.281	22.35	0.05	113.5
	(010) IP	1.590	3.95	0.447	12.7
Y6	(010) OOP	1.612	3.90	0.423	13.4
	(100) IP	0.257	24.44	0.089	63.9

Table S2 Photovoltaic parameters of devices based on BT-CAR2:Y6 under various optimization conditions.

Concentration	D:A by wt	SVA	V_{OC} (V)	J_{SC} (mA·cm^{-2})	FF (%)	PCE (%)
18 mg/ml	1:1	CB / 150s	0.841	25.29	68.53	14.58
20 mg/ml	**1:1**	**CB / 150s**	**0.836**	**25.96**	**68.62**	**14.90**
22 mg/ml	1:1	CB / 150s	0.835	25.91	68.07	14.73
20 mg/ml	1.2:1	CB / 150s	0.844	24.11	67.19	13.67
20 mg/ml	1:1.2	CB / 150s	0.833	25.98	67.74	14.66
20 mg/ml	1:1	/	0.882	19.88	41.58	7.29
20 mg/ml	1:1	CB / 120s	0.844	25.48	66.41	14.28
20 mg/ml	1:1	CB / 180s	0.826	26.17	67.15	14.52

Table S3 Photovoltaic parameters of devices based on BT-CAR4:Y6 under various optimization conditions.

Concentration	D:A by wt	SVA	V_{OC} (V)	J_{SC} (mA·cm^{-2})	FF (%)	PCE (%)
18 mg/ml	1:1	CB / 150s	0.846	25.22	71.60	15.28
20 mg/ml	**1:1**	**CB / 150s**	**0.846**	**25.83**	**71.05**	**15.52**
22 mg/ml	1:1	CB / 150s	0.840	26.21	69.23	15.24
20 mg/ml	1.2:1	CB / 150s	0.851	25.00	68.28	14.53
20 mg/ml	1:1.2	CB / 150s	0.843	25.75	70.63	15.33
20 mg/ml	1:1	/	0.889	22.11	43.60	8.57
20 mg/ml	1:1	CB / 120s	0.850	25.61	70.33	15.31
20 mg/ml	1:1	CB / 180s	0.836	26.02	70.47	15.33

Table S4 Photovoltaic parameters of devices based on BT-CAR6:Y6 under various optimization conditions.

Concentration	D:A by wt	SVA	V_{OC} (V)	J_{SC} (mA·cm^{-2})	FF (%)	PCE (%)
18 mg/ml	1:1	CB / 150s	0.836	24.13	72.62	14.65
20 mg/ml	**1:1**	**CB / 150s**	**0.834**	**25.09**	**72.86**	**15.24**
22 mg/ml	1:1	CB / 150s	0.832	25.20	70.27	14.73
20 mg/ml	1.2:1	CB / 150s	0.839	24.63	69.26	14.31
20 mg/ml	1:1.2	CB / 150s	0.831	25.34	71.50	15.06
20 mg/ml	1:1	/	0.888	22.02	43.93	8.59
20 mg/ml	1:1	CB / 120s	0.841	24.56	71.32	14.73
20 mg/ml	1:1	CB / 180s	0.827	25.61	70.00	14.83

Table S5 Photovoltaic parameters of devices based on BT-CAR2:Y6 under the best optimized conditions.

Concentration	D:A by wt	SVA	V_{OC} (V)	J_{SC} (mA·cm^{-2})	FF (%)	PCE (%)
20 mg/ml	1 : 1	CB / 150s	0.830	25.49	68.94	14.59
20 mg/ml	1 : 1	CB / 150s	0.836	25.53	69.02	14.72
20 mg/ml	1 : 1	CB / 150s	0.835	25.80	68.62	14.79
20 mg/ml	1 : 1	CB / 150s	0.829	25.49	68.59	14.49
20 mg/ml	1 : 1	CB / 150s	0.835	25.87	67.38	14.55
20 mg/ml	1 : 1	CB / 150s	0.837	25.91	66.91	14.50
20 mg/ml	1 : 1	CB / 150s	0.835	25.84	67.46	14.56
20 mg/ml	1 : 1	CB / 150s	0.839	25.77	68.50	14.82
20 mg/ml	1 : 1	CB / 150s	0.832	25.32	68.03	14.33
20 mg/ml	1 : 1	CB / 150s	0.839	25.50	68.50	14.66
20 mg/ml	1 : 1	CB / 150s	0.832	25.61	68.43	14.58
20 mg/ml	1 : 1	CB / 150s	0.830	25.46	69.49	14.68
20 mg/ml	1 : 1	CB / 150s	0.836	25.28	68.24	14.43
20 mg/ml	1 : 1	CB / 150s	0.835	25.84	68.42	14.75
20 mg/ml	1 : 1	CB / 150s	0.836	25.96	68.62	14.90

Table S6 Photovoltaic parameters of devices based on BT-CAR4:Y6 under the best optimized conditions.

Concentration	D:A by wt	SVA	V_{OC} (V)	J_{SC} (mA·cm^{-2})	FF (%)	PCE (%)
20 mg/ml	1 : 1	CB / 150s	0.845	25.36	71.08	15.24
20 mg/ml	1 : 1	CB / 150s	0.845	25.62	69.73	15.09
20 mg/ml	1 : 1	CB / 150s	0.846	25.80	70.07	15.29
20 mg/ml	1 : 1	CB / 150s	0.851	25.19	70.77	15.16
20 mg/ml	1 : 1	CB / 150s	0.840	25.20	70.83	15.00
20 mg/ml	1 : 1	CB / 150s	0.836	25.56	71.24	15.23
20 mg/ml	1 : 1	CB / 150s	0.842	25.21	71.31	15.13
20 mg/ml	1 : 1	CB / 150s	0.836	25.23	70.80	14.93
20 mg/ml	1 : 1	CB / 150s	0.835	25.51	71.53	15.23
20 mg/ml	1 : 1	CB / 150s	0.839	25.21	72.75	15.39
20 mg/ml	1 : 1	CB / 150s	0.835	25.18	71.92	15.13
20 mg/ml	1 : 1	CB / 150s	0.848	25.00	69.99	14.84
20 mg/ml	1 : 1	CB / 150s	0.845	25.63	70.59	15.30
20 mg/ml	1 : 1	CB / 150s	0.846	25.83	71.05	15.52
20 mg/ml	1 : 1	CB / 150s	0.835	25.65	70.50	15.09

Table S7 Photovoltaic parameters of devices based on BT-CAR6:Y6 under the best optimized conditions.

Concentration	D:A by wt	SVA	V_{OC} (V)	J_{SC} (mA·cm^{-2})	FF (%)	PCE (%)
20 mg/ml	1 : 1	CB / 150s	0.838	25.07	70.95	14.90
20 mg/ml	1 : 1	CB / 150s	0.831	25.09	71.27	14.86
20 mg/ml	1 : 1	CB / 150s	0.831	25.09	71.70	14.96
20 mg/ml	1 : 1	CB / 150s	0.832	24.30	71.42	14.44
20 mg/ml	1 : 1	CB / 150s	0.837	24.57	71.02	14.60
20 mg/ml	1 : 1	CB / 150s	0.839	24.80	71.15	14.81
20 mg/ml	1 : 1	CB / 150s	0.837	25.14	71.60	15.07
20 mg/ml	1 : 1	CB / 150s	0.834	25.09	72.86	15.24
20 mg/ml	1 : 1	CB / 150s	0.837	25.07	70.60	14.82
20 mg/ml	1 : 1	CB / 150s	0.825	24.71	72.28	14.73
20 mg/ml	1 : 1	CB / 150s	0.832	25.24	71.19	14.95
20 mg/ml	1 : 1	CB / 150s	0.840	24.65	71.70	14.84
20 mg/ml	1 : 1	CB / 150s	0.831	25.33	70.30	14.80
20 mg/ml	1 : 1	CB / 150s	0.834	24.96	70.72	14.73
20 mg/ml	1 : 1	CB / 150s	0.839	24.53	71.15	14.63

Table S8 Statistical sheet of PCEs of BTR-based ASM-OSCs (PCE > 13 %).

Time	Donor	Acceptor	V_{OC} (V)	J_{SC} (mA·cm^{-2})	FF (%)	PCE (%)	Ref.
2019	BSFTR	Y6	0.85	23.16	69.66	13.69	2
2019	BTR -Cl	Y6	0.86	24.17	65.5	13.61	3
2019	BTEC -2F	Y6	0.854	21.55	72.35	13.34	4
2020	SM1-F	Y6	0.87	23.25	69.9	14.07	5
2020	BT -2F	Y6	0.85	22.38	72.27	13.80	6
2020	BTTZR	Y6	0.88	23.2	68	13.90	7
2020	TBFT -TR	Y6	0.784	24.59	72.78	14.03	8
2021	FYSM - SiCl	Y6	0.85	23.7	66.8	13.40	9
2021	SL1	Y6	0.88	23.2	68	13.90	10
2021	BT-REH-Cl	Y6	0.867	22.93	69.86	13.90	11
2022	SM -CA -Reh	N3	0.84	25.42	77.5	16.34	12
2022	SM-CA	N3	0.838	24.33	75.62	15.4	12
2022	SM-Reh	N3	0.834	25.42	69.64	14.76	12
2022	BTR - SCl	Y6	0.88	23.4	70.8	14.60	13
2022	BDT-UF	N3	0.855	24.8	69.9	15.10	14
2022	BDT-DF	N3	0.854	24.3	68.8	14.5	14
2024	BT-CAR2	Y6	0.836	25.96	68.62	14.90	This Work
2024	BT-CAR4	Y6	0.846	25.83	71.05	15.52	This Work
2024	BT-CAR6	Y6	0.834	25.09	72.86	15.24	This Work

Table S9 The electron mobility (μ_e) and hole mobility (μ_h) values of the active layers

Active Layer	μ_h /×10^{-4} cm^2 V^{-1} s^{-1}(*a*)	μ_e/×10^{-4} cm^2 V^{-1} s^{-1} (*a*)	μ_e / μ_h
BT-CAR2:Y6	5.37±0.70	5.79±0.99	1.08
BT-CAR4:Y6	4.62±0.84	5.88±1.28	1.27
BT-CAR6:Y6	3.71±0.41	5.90±0.98	1.86

(*a*) Average mobility values and the deviations based on individual 9 cells.

Table S10 Contact angle (CA), surface tension, and Flory–Huggins interaction parameter (χ) of the used materials.

Material	Contact angle		γ^{p} (*a*)	γ^{d} (*b*)	γ (*c*)	$\chi^{D\text{-}A}$ (*d*)
	θ_{water} / °	$\theta_{diiodomethane}$ / °	/mN m^{-1}	/mN m^{-1}	/mN m^{-1}	
BT-CAR2	104.48	55.93	0.01	32.09	32.10	0.17κ
BT-CAR4	105.09	58.55	0.02	30.41	30.43	0.32κ
BT-CAR6	105.43	59.74	0.03	29.66	29.69	0.40κ
Y6	96.76	46.14	0.28	36.70	36.98	/

(*a*) Surface tension from polarity component. (*b*) Surface tension from dispersion component. (*c*) The total surface tension is calculated through the equation of $\gamma = \gamma^{p} + \gamma^{d}$. (*d*) The Flory-Huggins interaction parameter between the donor (D) and acceptor (A) is calculated with the equation of $\chi^{D\text{-}A} = \kappa (\sqrt{\gamma D} - \sqrt{\gamma A})^2$

Table S11 Summary of the GIWAXS parameters for the blend films

Compound	Peak	Position / $Å^{-1}$	D-spacing / Å	FWHM / $Å^{-1}$	Coherence length / Å
BT-CAR2:Y6	(100) OOP	0.28	22.43	0.074	76.8
	(100) IP	0.28	22.43	0.144	39.5
	(010) IP	1.685	3.73	0.572	9.9
BT-CAR4:Y6	(100) OOP	0.276	22.75	0.075	75.6
	(100) IP	0.285	22.04	0.157	36.1
	(010) IP	1.678	3.74	0.536	10.6
BT-CAR6:Y6	(100) OOP	0.271	23.17	0.069	82.4
	(100) IP	0.290	21.66	0.138	41.2
	(010) IP	1.655	3.79	0.590	9.6

Reference

1 S. Ye, T. Chen, J. Yu, S. Wang, S. Li, J. Wang, Y. Fu, Y. Zhu, M. Wang, X. Lu, Z. Ma, C.-Z. Li, M. Shi and H. Chen, *Energy Environ. Sci.*, 2024, **17**, 5137-5146.

2 Q. Yue, H. Wu, Z. Zhou, M. Zhang, F. Liu and X. Zhu, *Advanced Materials*, 2019, **31**, 1904283.

3 H. Chen, D. Hu, Q. Yang, J. Gao, J. Fu, K. Yang, H. He, S. Chen, Z. Kan, T. Duan, C. Yang, J. Ouyang, Z. Xiao, K. Sun, S. Lu, *Joule*, 2019, **3**, 3034–3047.

4 J. Ge, L. Xie, R. Peng, B. Fanady, J. Huang, W. Song, T. Yan, W. Zhang and Z. Ge, *Angewandte Chemie International Edition*, 2020, **59**, 2808–2815.

5 B. Qiu, Z. Chen, S. Qin, J. Yao, W. Huang, L. Meng, H. Zhu, Y. (Michael) Yang, Z.-G. Zhang and Y. Li, *Advanced Materials*, 2020, **32**, 1908373.

6 J. Gao, J. Ge, R. Peng, C. Liu, L. Cao, D. Zhang, B. Fanady, L. Hong, E. Zhou and Z. Ge, *J. Mater. Chem. A*, 2020, **8**, 7405–7411.

7 Y. Wang, Y. Wang, L. Zhu, H. Liu, J. Fang, X. Guo, F. Liu, Z. Tang, M. Zhang and Y. Li, *Energy Environ. Sci.*, 2020, **13**, 1309–1317.

8 R. Sun, Y. Wu, J. Guo, Z. Luo, C. Yang and J. Min, *Sci. China Chem.*, 2020, **63**, 1246–1255.

9 W. Su, Y. Wang, Z. Yin, Q. Fan, X. Guo, L. Yu, Y. Li, L. Hou, M. Zhang, Q. Peng, Y. Li and E. Wang, *ChemSusChem*, 2021, **14**, 3535–3543.

10 Y. Wang, Q. Fan, Y. Wang, J. Fang, Q. Liu, L. Zhu, J. Qiu, X. Guo, F. Liu, W. Su and M. Zhang, *Chinese Journal of Chemistry*, 2021, **39**, 2147–2153.

11 H. Chen, H. Tang, D. Hu, Y. Xiao, J. Fu, J. Lv, Q. Yu, Z. Xiao, X. Lu, H. Hu and S. Lu, *Energies*, 2021, **14**, 2505.

12 J. Ge, L. Hong, H. Ma, Q. Ye, Y. Chen, L. Xie, W. Song, D. Li, Z. Chen, K. Yu, J. Zhang, Z. Wei, F. Huang and Z. Ge, *Advanced Materials*, 2022, **34**, 2202752.

13 H. Liang, Y. Wang, X. Guo, D. Yang, X. Xia, J. Wang, L. Zhang, Y. Shi, X. Lu and M. Zhang, *J. Mater. Chem. A*, 2022, **10**, 10926–10934.

14 Q. Ye, J. Ge, D. Li, Z. Chen, J. Shi, X. Zhang, E. Zhou, D. Yang and Z. Ge, *ACS Appl. Mater. Interfaces*, 2022, **14**, 33234–33241.